MCR RapidIMPACT

Molecular Cancer Research

Whole-Genome and Transcriptional Analysis of Treatment-Emergent Small-Cell Neuroendocrine Prostate Cancer Demonstrates Intraclass Heterogeneity

Rahul R. Aggarwal[1], David A. Quigley[1], Jiaoti Huang[2], Li Zhang[1], Tomasz M. Beer[3], Matthew B. Rettig[4], Rob E. Reiter[4], Martin E. Gleave[5], George V. Thomas[3], Adam Foye[1], Denise Playdle[1], Paul Lloyd[1], Kim N. Chi[5], Christopher P. Evans[6], Primo N. Lara[6], Felix Y. Feng[1], Joshi J. Alumkal[3], and Eric J. Small[1]

Abstract

Therapeutic resistance in metastatic castration-resistant prostate cancer (mCRPC) can be accompanied by treatment-emergent small-cell neuroendocrine carcinoma (t-SCNC), a morphologically distinct subtype. We performed integrative whole-genome and -transcriptome analysis of mCRPC tumor biopsies including paired biopsies after progression, and multiple samples from the same individual. t-SCNC was significantly less likely to have amplification of *AR* or an intergenic *AR*-enhancer locus, and demonstrated lower expression of *AR* and its downstream transcriptional targets. Genomic and transcriptional hallmarks of t-SCNC included biallelic loss of *RB1*, elevated expression levels of *CDKN2A* and *E2F1*, and loss of expression of the *AR* and *AR*-responsive genes including *TMPRSS2* and *NKX3-1*. We identified three tumors that converted from adenocarcinoma to t-SCNC and demonstrate spatial and temporal intrapatient heterogeneity of metastatic tumors harboring adenocarcinoma, t-SCNC, or mixed expression phenotypes, with implications for treatment strategies in which dual targeting of adenocarcinoma and t-SCNC phenotypes may be necessary.

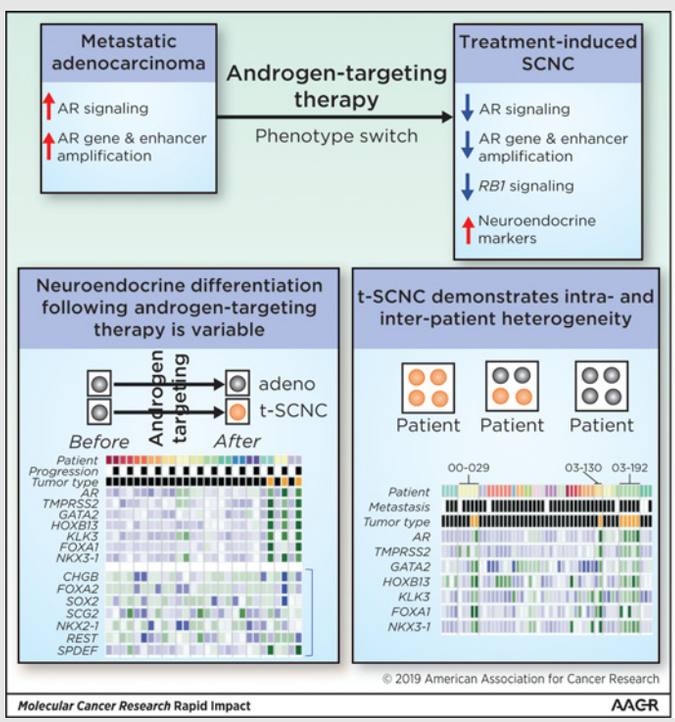

Implications: The t-SCNC phenotype is characterized by lack of *AR* enhancer gain and loss of *RB1* function, and demonstrates both interindividual and intraindividual heterogeneity.

Visual Overview: http://mcr.aacrjournals.org/content/molcanres/17/6/1235/F1.large.jpg.

[1]University of California San Francisco, San Francisco, California. [2]Duke University, Durham, North Carolina. [3]Oregon Health & Science University, Portland, Oregon. [4]University of California Los Angeles, Los Angeles, California. [5]Vancouver Prostate Centre, University of British Columbia, Vancouver, British Columbia, Canada. [6]University of California Davis, Davis, California.

Note: Supplementary data for this article are available at Molecular Cancer Research Online (http://mcr.aacrjournals.org/).

R.R. Aggarwal and D.A. Quigley are co-primary authors of this article.

F.Y. Feng, J.J. Alumkal, and E.J. Small are co-senior authors of this article.

Corresponding Author: Rahul R. Aggarwal, University of California, San Francisco, 1600 Divisadero Street, Room A717, Box 1711, San Francisco, CA 94143-1711. Phone: 415-353-9278; Fax: 415-353-7779; E-mail: Rahul.Aggarwal@ucsf.edu

Mol Cancer Res 2019;17:1235–40

doi: 10.1158/1541-7786.MCR-18-1101

Introduction

Metastatic castration-resistant prostate cancer (mCRPC) is a clinically and genomically heterogeneous disease entity with widely varying outcomes (1, 2). Small-cell neuroendocrine cancer is a highly lethal subset of prostate cancer that is rare at the time of diagnosis but increasingly common upon emergence of resistance to androgen receptor (AR)-targeted therapies (3–6). Targeted and whole-exome sequencing of treatment-emergent small-cell neuroendocrine prostate cancer (t-SCNC) demonstrates frequent inactivating mutations and/or copy number loss of *RB1* and *TP53* (3). However the exome represents a small percentage of the genome, and the complete genomic landscape of t-SCNC, along with the impact on downstream transcriptional profile, remain to be elucidated.

Whole-genome sequencing (WGS) methods have identified key structural variants present in mCRPC, including amplification of an upstream enhancer of *AR* that drives AR expression and contributes to progression of castration-resistant disease (7–9). Whether t-SCNC harbors structural variants, and whether this has downstream implications for disease progression from adenocarcinoma to t-SCNC is not known. We previously interrogated the whole genomes and transcriptomes of 101 mCRPC samples (7), and have subsequently used unbiased clustering to identify the subgroup of tumors harboring a t-SCNC gene expression signature (10). We then contrasted the genomic hallmarks of tumors harboring t-SCNC expression signatures with those that did not, including the presence of *AR* enhancer amplification, confirming our observations using a previously published mCRPC cohort (5). We next extended these results to evaluate the gene expression profile of 14 metastatic paired biopsies obtained at baseline and progression from our recently published cohort (6) to identify changes in expression patterns associated with the transition from adenocarcinoma to t-SCNC. Finally, we interrogated a published mCRPC cohort that assayed multiple distinct metastatic sites per individual (6) and demonstrated frequent intraindividual heterogeneity in t-SCNC.

Materials and Methods

Case selection and sample preparation

Patient tissue samples were obtained through the Stand Up 2 Cancer/Prostate Cancer Foundation-funded West Coast Prostate Cancer Dream Team project, a prospective, multi-center study that acquired metastatic CRPC biopsies from five investigational sites (11). Patients were required to have histologic evidence of prostate adenocarcinoma at the time of diagnosis, with subsequent development of mCRPC, and at least one metastatic lesion accessible for image-guided percutaneous biopsy. Human studies were approved and overseen by Institutional Review Board of the participating institutions. All individuals provided written informed consent to participate in the prospective tissue acquisition protocol including molecular profiling of tumor and germline samples.

Details of patient sample preparation have been reported previously (7, 10). Briefly, samples were obtained using image-guided core needle biopsy of metastatic lesion in the bone or soft tissue. Separate cores were obtained and freshly frozen for DNA/RNA sequencing and formalin-fixed, paraffin-embedded for histologic determination of adenocarcinoma versus t-SCNC morphology, as described previously (7, 10). Tumor structural variation and copy number data were ascertained by WGS as described previously (7). Data from previously published studies (5, 6) were downloaded from cBioPortal (http://cbioportal.org).

Statistical analyses

All statistical analysis was performed using R (v3.3.3). Between-group comparisons of continuous variables were performed with the Wilcoxon rank sum test. Contingency table tests were performed with Fisher exact test.

Results

Unbiased clustering of expression profile identifies t-SCNC subset

Unbiased gene expression clustering of 101 samples in the WGS cohort identified a previously reported subset of five samples (10) that bore a t-SCNC expression signature, with low to absent expression of AR signaling, elevated expression of genes associated with small-cell morphology, elevated expression of *E2F1* and *CDKN2A*, low expression of *NOTCH2*/*NOTCH2NL*, and elevated expression of the *ASCL1*, a transcription factor essential for neural development (ref. 12; Fig. 1A). t-SCNC samples often harbored elevated expression of the *ETV1*, *ETV4*, and *ETV5* in the absence of activating ETS-family gene fusions; these transcription factors play an important role in neural development (13, 14). Clinical features of the cohort are shown in Supplementary Table S1. We compared these results with a previously published analysis of mCRPC and neuroendocrine tumors (ref. 5; Fig. 1B). A gene set reported by Beltran and colleagues to distinguish adenocarcinoma and neuroendocrine tumors separated WGS t-SCNC and neuroendocrine samples (ref. 5; Supplementary Fig. S1), confirming the neuroendocrine phenotype of the t-SCNC samples. WGS and Beltran t-SCNC tumors consistently lost *AR* gene expression. We observed that Beltran tumors exhibited uniform loss of *AR* signaling but a gradient of *RB1* and neuroendocrine marker expression, suggesting neuroendocrine tumors can harbor a heterogeneous expression phenotype.

Molecular correlates of the t-SCNC phenotype

We then searched genome wide for associations between the t-SCNC expression phenotype and somatic alterations by WGS. As reported previously (5), tumors harboring the t-SCNC expression phenotype were less likely to bear *AR* gene locus DNA amplification than samples with an adenocarcinoma expression phenotype (2 of 5; 40% vs. 69 of 96; 72%). In addition, we observed t-SCNC tumors were significantly less likely to harbor *AR* enhancer amplification (1 of 5; 20% vs. 80 of 96; 83%, $P = 0.005$). The two WGS t-SCNC samples with *AR* gene locus DNA amplification had significantly lower AR expression levels than other samples bearing *AR* amplification, with one sample (DTB-205) showing negligible expression of AR, compatible with complete silencing of AR expression despite the presence of a DNA copy number increase at the *AR* locus. Samples with the t-SCNC expression phenotype were significantly more likely to harbor bi-allelic *RB1* inactivation (3 of 5; 60% vs. 9 of 96; 9.4% $P = 0.01$). The two t-SCNC samples without bi-allelic *RB1* inactivation harbored mono-allelic *RB1* inactivation. We observed a significant association between *RB1* expression levels and the number of predicted functional *RB1* alleles, compatible with a

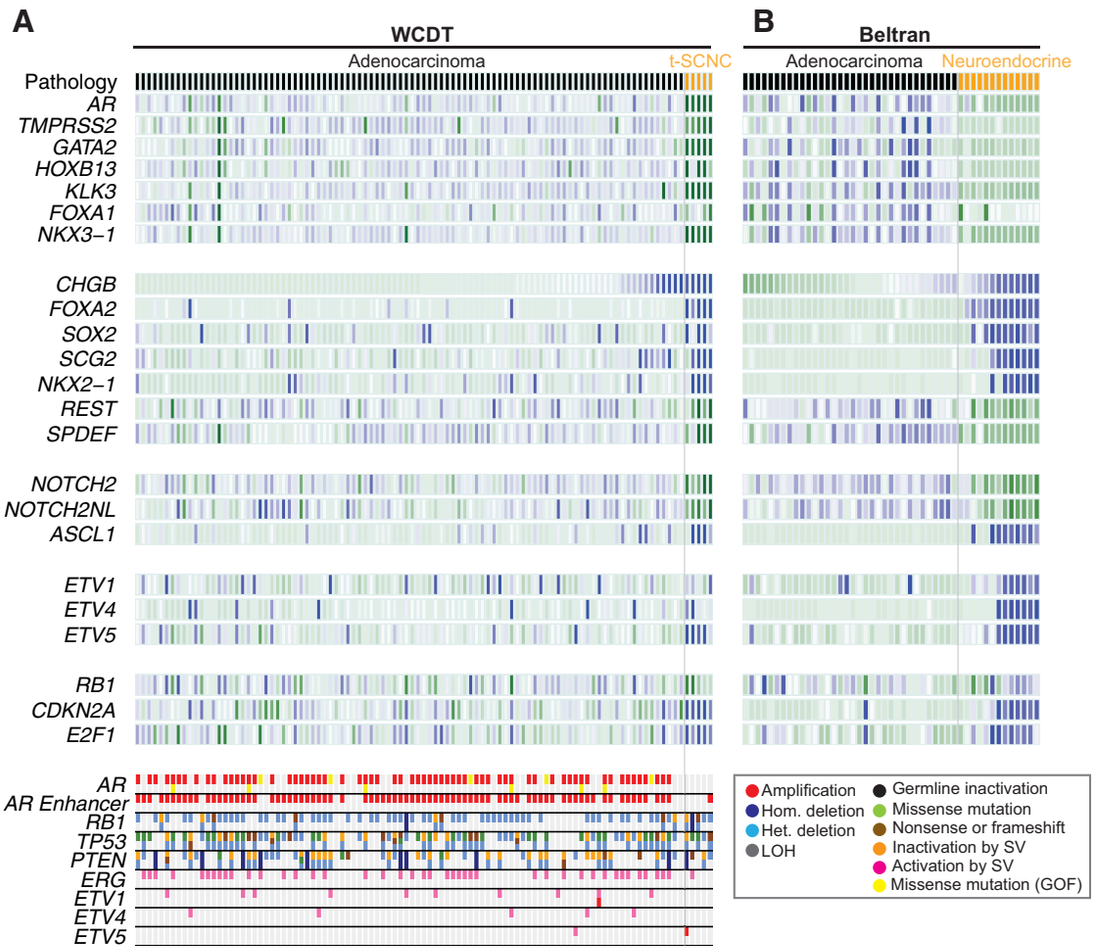

Figure 1.

Expression correlates of t-SCNC status. **A,** Heatmap showing expression of selected genes in the WGS cohort differentially expressed between t-SCNC and adenocarcinoma expression phenotypes, where darker blue/green indicate higher/lower expression. Adenocarcinoma/t-SCNC status assessed by gene expression profile is indicated by black/orange bar in top row (top). Somatic variants detected by WGS in key prostate cancer driver and tumor suppressor genes. The frequency of *AR*-enhancer amplification was lower, and *RB1* bi-allelic loss higher in t-SCNC versus adenocarcinoma samples ($P < 0.05$ for both comparisons; bottom). **B,** Heatmap showing expression of genes in **A** in the Beltran dataset (5). Samples designated CRPC-ADENO/CRPC-NEPC in that publication are indicated by black/orange bar in top row. GOF, gain of function; Hom, homogeneous; Het, heterogeneous; SV, structural variation; WCDT, West Coast Dream Team.

dose effect of allelic loss (Fig. 2A). All t-SCNC samples had significantly lower expression of *RB1* ($P = 0.003$) and significantly higher expression of *CDKN2A* and *E2F1* ($P = 0.0002$, 0.0004, respectively) compared with samples with an adenocarcinoma expression phenotype, consistent with genetic inactivation of *RB1* (Fig. 2B). Application of a validated *RB1* loss gene expression signature (6) likewise demonstrated significant enrichment in the t-SCNC samples (mean *RB1* loss score of 3.79 in t-SCNC vs. −1.16 in samples with adenocarcinoma expression phenotype, $P = 0.009$). No other recurrent structural variant was significantly associated with the t-SCNC expression phenotype. Bi-allelic *TP53* inactivation was present in three of five tumors with the t-SCNC expression phenotype (60%) versus 43 of 96 adenocarcinoma samples (45%; $P > 0.05$; Fig. 1A). Likewise, bi-allelic *PTEN* inactivation was present in two of five tumors with t-SCNC phenotype (40%) versus 33 of 96 adenocarcinoma samples (34%).

Conversion to t-SCNC may be a late onset event in mCRPC

The timing and mechanism of conversion from adenocarcinoma to t-SCNC during the course of AR-targeting therapies and progression from castration-sensitive to castration-resistant disease remains to be elucidated. To begin to address this question, we identified 14 patients in our previously published cohort (6) of patients who had RNA-seq data available from mCRPC biopsies obtained at two time points (baseline and progression). The clinical characteristics of these patients are shown in Supplementary Table S2. In 11 of the 14 patients, both baseline and progression biopsies had an adenocarcinoma gene expression profile (Fig. 2B, left). Three patients (DTB-080, DTB-135, and DTB-210) had an adenocarcinoma expression phenotype in their baseline sample and t-SCNC expression profile at progression (Fig. 2B, right). The previously published neuroendocrine gene set readily distinguished the three progression t-SCNC tumors in this analysis from the adenocarcinoma samples (Supplementary

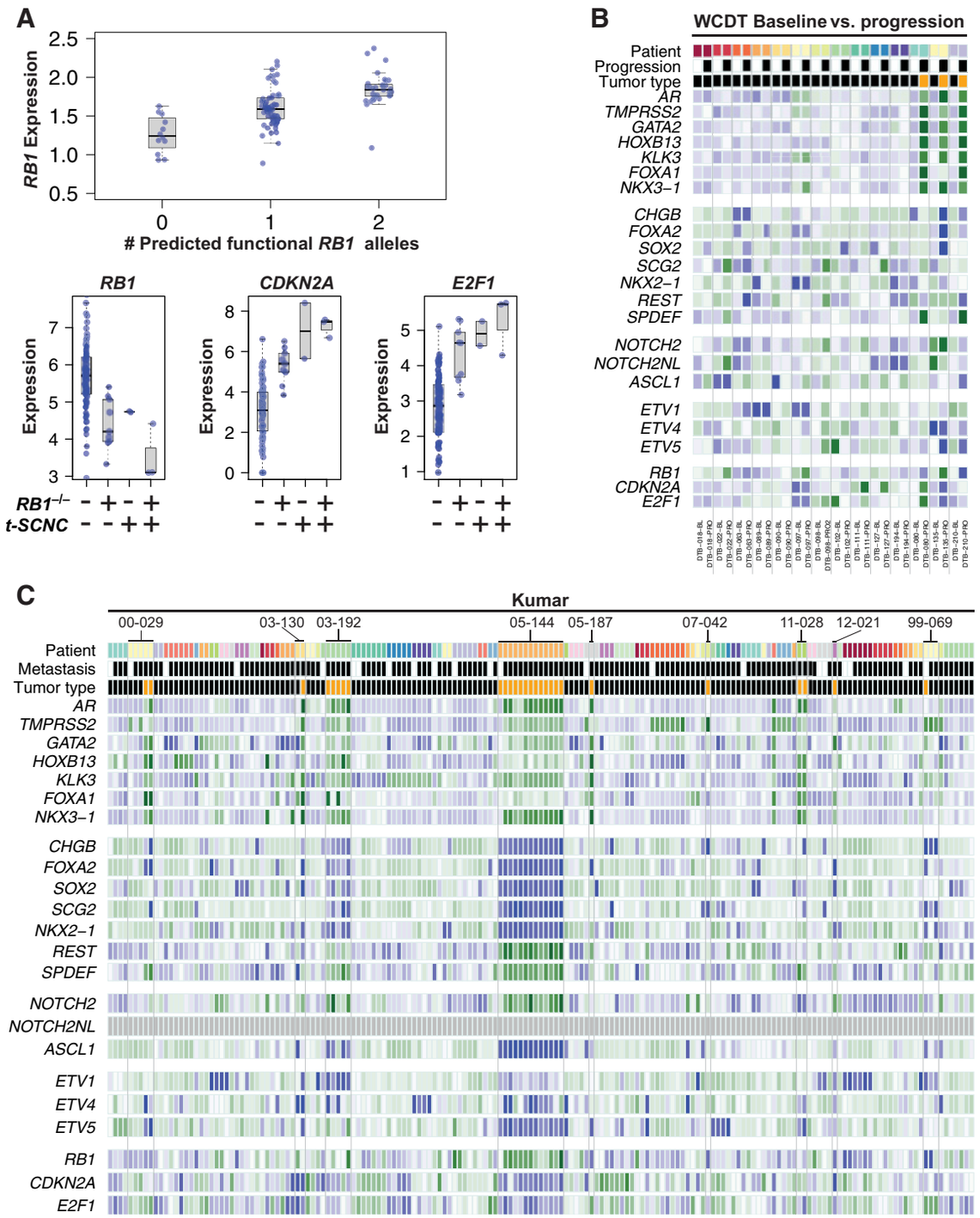

Figure 2.

RB pathway expression is associated with t-SCNC status. **A,** Expression of *RB1* is significantly associated with the number of predicted functional alleles (top). Expression of *RB1, CDKN2A*, and *E2F1* were significantly different in $RB1^{-/-}$ and t-SCNC tumors compared with $RB1^{+/+}$ tumors with adenocarcinoma expression phenotype (bottom). **B,** Heatmap showing expression of NEPC genes in paired West Coast Dream Team (WCDT) baseline and progression mCRPC samples. Tumors from the same patient are indicated by a common color on the top line and set off by vertical lines. Baseline/progression status is indicated by white/black bar in second row. Adenocarcinoma/t-SCNC status assessed by gene expression profile is indicated by black/orange bar in third row. **C,** Heatmap showing expression of NEPC genes in primary, localized, and mCRPC samples from Kumar dataset (6). All tumors from the same patient are indicated by a common color on the top line. Samples derived from primary/metastatic lesions are indicated by white/black on the second line. Adenocarcinoma/t-SCNC status assessed by gene expression profile is indicated by black/orange bar in third row.

Fig. S1). The median duration of androgen signaling inhibitor therapy between baseline and progression biopsies did not differ between those with t-SCNC at progression versus those without (median duration 6.7 months vs. 9.5 months; $P = 0.13$). In the case of patients DTB-080 and DTB-210, both the baseline and progression biopsy samples were derived from the same lesion (in bone and lymph node, respectively). Paired samples from patient DTB-135 were obtained from adjacent lymph nodes in the same anatomic region. We observed consistent *AR* signaling loss and a gradient of small-cell expression in the progression samples, ranging from very strong (DTB-135) to weak (DTB-080), further evidence of intraclass heterogeneity within t-SCNC.

To further assess intrapatient heterogeneity of the t-SCNC phenotype, we then reanalyzed a previously published cohort of 176 primary and metastatic prostate tumors (6). The investigators of this autopsy series, wherein most patients contributed more than one tumor sample, had reported that in most cases a single metastasis was representative of all tumors present in a given patient. We confirmed that, as previously reported, all metastatic tumors from patients 03-192 ($N = 5$) and 05-144 ($N = 12$) harbored the neuroendocrine prostate cancer (NEPC) phenotype (Fig. 2C). However, we also noted patients with metastases harboring both t-SCNC and adenocarcinoma phenotypes (patients 00-029, 03-130, 05-187, and 07-042). The neuroendocrine gene set distinguished t-SCNC and adenocarcinoma tumors in these samples, and confirmed the neuroendocrine expression phenotype of t-SCNC tumors that diverged in phenotype from adenocarcinomas within a given patient (Supplementary Fig. S1). We conclude that both the adenocarcinoma and neuroendocrine phenotypes can be present in distinct metastatic lesions within in the same patient, compatible with this phenotype arising after the independent establishment of physically distinct metastatic lesions.

Discussion

In this article we describe the structural variants of t-SCNC, a highly lethal variant of mCRPC, and how they differ from adenocarcinoma tumors. We undertook an unbiased clustering approach of the transcriptome to independently identify a subset of tumors harboring a t-SCNC expression profile and confirmed this classification using a previously published gene signature of NEPC (5). We observed a near mutual exclusivity with *AR*-enhancer amplification, which has recently been reported to be present in up to 80% of mCRPC biopsies that do not harbor t-SCNC (7). This finding, coupled with the enrichment of *RB1* loss, distinguished t-SCNC from mCRPC without transcriptional features of small cell/neuroendocrine transformation. Using serial biopsies, we demonstrate temporal heterogeneity of t-SCNC differentiation arising in patients with established mCRPC. Based upon independent analysis of a previously published dataset, we demonstrate spatial heterogeneity of t-SCNC differentiation across metastatic lesions within an individual patient.

We and others have previously demonstrated that t-SCNC harbors lower canonical *AR* transcriptional output, yet with retained AR protein expression (10). The results of this analysis build upon these previous findings by virtue of whole-genome interrogation and the finding of lower prevalence of amplification of upstream enhancer of AR. Notably, even in the two cases of t-SCNC with amplification of the *AR* gene locus or upstream enhancer, respectively, we observed lower expression of *AR* and its downstream transcriptional targets. This is consistent with a characterization of an *AR* "indifferent state", and suggests that epigenetic dysregulation is a hallmark of t-SCNC (15). Further study of the epigenetic landscape of t-SCNC will be required to ascertain the mechanisms underpinning the putative silencing of canonical AR-driven transcription.

In a pair-wise comparison of the transcriptional profile of biopsies obtained at two time points in patients with mCRPC, we observed the emergence of t-SCNC at progression in 3 patients. These observations, although preliminary given the limited sample size, are consistent with a model where t-SCNC develops late during progression, after the onset of mCRPC and may be enriched following the use of second-generation androgen-signaling inhibitors (5). Whether the process driving the emergence of t-SCNC is related to transdifferentiation from an adenocarcinoma precursor versus clonal expansion remains to be defined. Further prospective studies in patients with mCRPC with serial genomic and transcriptomic assessment at various time points are needed to delineate the kinetics and mechanism underpinning the emergence of t-SCNC.

Previously, our group and others demonstrated that loss of function of tumor suppressors *RB1*, *TP53*, and *PTEN* are hallmarks of small-cell NEPC (3, 6). Mechanistic studies have demonstrated that RB1- and TP53-deficient prostate cancer leads to lineage plasticity and resistance to antiandrogen therapy (16–18). Loss of two or more of the three tumor suppressors has been shown to lead to worse treatment outcomes in a prior study and in preclinical models (3, 19). In this analysis of the whole genome, *RB1* loss stands out as the key genomic hallmark of t-SCNC, leading to upregulation of E2F1 and acceleration of cell-cycle progression. *TP53* loss may promote a different genotype and phenotype than *RB1* loss, characterized by marked frequency of inversions and chromothripsis (7). Further interrogation of individual loss of each of these tumor suppressor genes is required to delineate specific effects on pathogenesis of t-SCNC and treatment outcomes.

Our finding of interpatient heterogeneity in the gradient of t-SCNC expression, together with intrapatient spatial and temporal heterogeneity of adenocarcinoma versus t-SCNC differentiation demonstrated in our dataset and others, has implications for the development of therapeutic strategies in this setting. Successful treatment of t-SCNC may require dual targeting with continuation of treatments aimed at blocking adenocarcinoma targets including the AR. The gradient of t-SCNC expression suggests plasticity in the emergence of this phenotype, and underscores the potential for epigenetically mediated reversal of t-SCNC differentiation and restoring dependence on the AR. These strategies warrant prospective evaluation as novel targets and targeted therapies are evaluated in t-SCNC.

Disclosure of Potential Conflicts of Interest

T.M Beer reports receiving commercial research grants from Alliance Foundation Trials, Boehringer Ingelheim, Corcept Therapeutics, Janssen Research & Development, Medivation/Astellas, OncoGenex, Sotio, and Theraclone Sciences/OncoResponse, has ownership interest (including stock, patents, etc.) in Salarius Pharmaceuticals, and is a consultant/advisory board member for AbbVie, AstraZeneca, Pfizer, Astellas Pharma, Bayer, Boehringer Ingelheim, Clovis Oncology, GlaxoSmithKline, Janssen Biotech, Janssen Japan, and Merck. M.B. Rettig reports receiving commercial research grants from Novartis, Johnson & Johnson, and Astellas, has received speakers bureau honoraria from, and is a consultant/advisory board member for Johnson & Johnson. G.V Thomas is a consultant/advisory board member for Auron Therapeutics. P. Lloyd is an

employee at Bluestar Genomics and has ownership interest (including stock, patents, etc.) in Bluestar Genomics, Pfizer, and Gilead. F.Y. Feng is co-founder at PFS Genomics and is a consultant/advisory board member for Astellas, Janssen, Sanofi, Bayer, Dendreon, Ferring, Celgene, and Blue Earth. J.J. Alumkal is a consultant/advisory board member for Astellas, Bayer, and Janssen. E.J. Small has ownership interest (including stock, patents, etc.) in Fortis Therapeutics and Harpoon Therapeutics and is a consultant/advisory board member for Janssen, Fortis Therapeutics, Harpoon Therapeutics, and Beigene. No potential conflicts of interest were disclosed by the other authors.

Authors' Contributions

Conception and design: R.R. Aggarwal, D.A. Quigley, J. Huang, T.M. Beer, M.B. Rettig, R.E. Reiter, M.E. Gleave, A. Foye, D. Playdle, C.P. Evans, F.Y. Feng, J.J. Alumkal, E.J. Small

Development of methodology: R.R. Aggarwal, J. Huang, T.M. Beer, A. Foye, D. Playdle, E.J. Small

Acquisition of data (provided animals, acquired and managed patients, provided facilities, etc.): R.R. Aggarwal, J. Huang, T.M. Beer, M.B. Rettig, R.E. Reiter, M.E. Gleave, G.V. Thomas, A. Foye, D. Playdle, P. Lloyd, K.N. Chi, C.P. Evans, P.N. Lara, J.J. Alumkal, E.J. Small

Analysis and interpretation of data (e.g., statistical analysis, biostatistics, computational analysis): R.R. Aggarwal, D.A. Quigley, J. Huang, L. Zhang, T.M. Beer, A. Foye, P. Lloyd, F.Y. Feng, J.J. Alumkal

Writing, review, and/or revision of the manuscript: R.R. Aggarwal, D.A. Quigley, J. Huang, L. Zhang, T.M. Beer, M.B. Rettig, R.E. Reiter, M.E. Gleave, A. Foye, K.N. Chi, C.P. Evans, P.N. Lara, F.Y. Feng, J.J. Alumkal, E.J. Small

Administrative, technical, or material support (i.e., reporting or organizing data, constructing databases): A. Foye, D. Playdle, P. Lloyd, F.Y. Feng

Study supervision: R.R. Aggarwal, T.M. Beer, R.E. Reiter, P.N. Lara, F.Y. Feng, J.J. Alumkal, E.J. Small

Acknowledgments

This research work was supported by a Stand Up To Cancer-Prostate Cancer Foundation Dream Team-Prostate Dream Team Translational Research Grant (SU2C-AACR-DT0812). This research grant is made possible by the generous support of the Movember Foundation. Stand Up to Cancer is a division of the Entertainment Industry Foundation. Research grants are administered by the American Association for Cancer Research, the Scientific Partner of SU2C. This work is also supported by; U.S. Army Department of Defense Prostate Cancer Program Impact Award (W81XWH-16-1-0495 to E.J. Small); Prostate Cancer Foundation Special Challenge Award (15CHAS03 to E.J. Small); Prostate Cancer Foundation Young Investigator Award (to D.A. Quigley); and Pacific Northwest Prostate Cancer SPORE/NCI (P50 CA 09186 to J.J. Alumkal).

The costs of publication of this article were defrayed in part by the payment of page charges. This article must therefore be hereby marked *advertisement* in accordance with 18 U.S.C. Section 1734 solely to indicate this fact.

Received October 17, 2018; revised December 9, 2018; accepted March 22, 2019; published first March 27, 2019.

References

1. Robinson D, Van Allen EM, Wu YM, Schultz N, Lonigro RJ, Mosquera JM, et al. Integrative clinical genomics of advanced prostate cancer. Cell 2015; 161:1215–28.
2. Ryan CJ, Smith MR, de Bono JS, Molina A, Logothetis CJ, de Souza P, et al. Abiraterone in metastatic prostate cancer without previous chemotherapy. N Engl J Med 2013;368:138–48.
3. Aparicio AM, Shen L, Tapia EL, Lu JF, Chen HC, Zhang J, et al. Combined tumor suppressor defects characterize clinically defined aggressive variant prostate cancers. Clin Cancer Res 2016;22:1520–30.
4. Beltran H, Rickman DS, Park K, Chae SS, Sboner A, MacDonald TY, et al. Molecular characterization of neuroendocrine prostate cancer and identification of new drug targets. Cancer Discov 2011;1:487–95.
5. Beltran H, Prandi D, Mosquera JM, Benelli M, Puca L, Cyrta J, et al. Divergent clonal evolution of castration-resistant neuroendocrine prostate cancer. Nat Med 2016;22:298–305.
6. Kumar A, Coleman I, Morrissey C, Zhang X, True LD, Gulati R, et al. Substantial interindividual and limited intraindividual genomic diversity among tumors from men with metastatic prostate cancer. Nat Med 2016; 22:369–78.
7. Quigley DA, Dang HX, Zhao SG, Lloyd P, Aggarwal R, Alumkal JJ, et al. Genomic hallmarks and structural variation in metastatic prostate cancer. Cell 2018;174:758–69.
8. Takeda DY, Spisák S, Seo JH, Bell C, O'Connor E, Korthauer K, et al. A somatically acquired enhancer of the androgen receptor is a noncoding driver in advanced prostate cancer. Cell 2018;174:422–32.
9. Viswanathan SR, Ha G, Hoff AM, Wala JA, Carrot-Zhang J, Whelan CW, et al. Structural alterations driving castration-resistant prostate cancer revealed by linked-read genome sequencing. Cell 2018;174:433–47.
10. Aggarwal R, Huang J, Alumkal JJ, Zhang L, Feng FY, Thomas GV, et al. Clinical and genomic characterization of treatment-emergent small-cell neuroendocrine prostate cancer: a multi-institutional prospective study. J Clin Oncol 2018;36:2492–503.
11. Aggarwal R, Beer TM, Gleave M, Stuart JM, Rettig M, Evans CP, et al. Targeting adaptive pathways in metastatic treatment-resistant prostate cancer: update on the Stand Up 2 Cancer/Prostate Cancer Foundation-Supported West Coast Prostate Cancer Dream Team. Eur Urol Focus 2016; 2:469–71.
12. Guillemot F, Lo LC, Johnson JE, Auerbach A, Anderson DJ, Joyner AL. Mammalian achaete-scute homolog 1 is required for the early development of olfactory and autonomic neurons. Cell 1993;75:463–76.
13. Paratore C, Brugnoli G, Lee HY, Suter U, Sommer L. The role of the Ets domain transcription factor Erm in modulating differentiation of neural crest stem cells. Dev Biol 2002;250:168–80.
14. Lin JH, Saito T, Anderson DJ, Lance-Jones C, Jessell TM, Arber S. Functionally related motor neuron pool and muscle sensory afferent subtypes defined by coordinate ETS gene expression. Cell 1998;95:393–407.
15. Chen R, Dong X, Gleave M. Molecular model for neuroendocrine prostate cancer progression. BJU Int 2018;122:560–70.
16. Ku SY, Rosario S, Wang Y, Mu P, Seshadri M, Goodrich ZW, et al. Rb1 and Trp53 cooperate to suppress prostate cancer lineage plasticity, metastasis, and antiandrogen resistance. Science 2017;355:78–83.
17. Mu P, Zhang Z, Benelli M, Karthaus WR, Hoover E, Chen CC, et al. SOX2 promotes lineage plasticity and antiandrogen resistance in TP53- and RB1-deficient prostate cancer. Science 2017;355:84–8.
18. Park JW, Lee JK, Sheu KM, Wang L, Balanis NG, Nguyen K, et al. Reprogramming normal human epithelial tissues to a common, lethal neuroendocrine cancer lineage. Science 2018;362:91–5.
19. Zou M, Toivanen R, Mitrofanova A, Floch N, Hayati S, Sun Y, et al. Transdifferentiation as a mechanism of treatment resistance in a mouse model of castration-resistant prostate cancer. Cancer Discov 2017;7:736–49.